

Chapter  
Chapter

4

Transient desorption of HD and D<sub>2</sub>  
molecules from the D/Si(100) surfaces  
exposed to a modulated H-beam

In this chapter, I will discuss the modulated H-beam induced transient desorption of HD and D<sub>2</sub> from the D/Si(100) surfaces. Since the surface structure of D/Si(110) is not well understood as reported in section 1.4 of Chapter 1, D/Si(100) surface have been chosen to measure the reaction lifetimes of desorbed components. The role of surface structure on reaction lifetimes of HD and D<sub>2</sub> components are also studied. By exposing the D/Si(100) surface to a modulated H-beam, Rahman et al.<sup>1</sup> reported that HD desorption is prompt in nature. On the other hand, D<sub>2</sub> desorption is composed of both fast and slow components. Recently, Inanaga *et.al.*<sup>2</sup> analyzed the AID rate curves,  $F(t)$  showing several components characterized with specific reaction lifetimes. In order to evaluate these reaction lifetimes, they defined the desorption probability function,  $\xi(t)$ ,

$$\xi(t) = \sum_i c_i e^{-\frac{t}{\tau_i}}, \quad (1)$$

where,  $c_i$  and  $\tau_i$  are the intensity and the reaction lifetime of the  $i$ -th component, respectively. Hence,  $F(t)$  could be expressed as a convolution of  $\xi(t)$  under the application of H-impulse function  $\eta(t)$ ,

$$F(t) = \int_0^t \xi(t-t')\eta(t')dt' \quad (2)$$

As a result of the best curve fitting, Inanaga et al. determined lifetimes of H induced HD and D<sub>2</sub> on the Si(100) surfaces by using a chopper rotating at 0.1 Hz. However, the

chopper had been suffered from a long rising- and falling-time ( $\approx 0.1$  s) and might be unable to detect true lifetimes of HD and fastest  $D_2$  component. In this experiments, I use a chopper rotating at 0.5 Hz with a shorter rising- and falling-time of  $\approx 0.02$  s and measured the lifetimes of HD and  $D_2$  channels. After analyzing rate curves of HD and  $D_2$ , it is found that, HD lifetime is 0.005 s, and  $D_2$  desorption rate is composed of four components with lifetimes of 0.005, 0.06, 0.8 and 30s. I propose here the atomistic mechanism based on the hot-complex (HC) model and explained the role of surface structure on the lifetimes of  $D_2$  components.

## 4.1 Experiment

Monolayer (dideuteride free) and saturated (dideuteride rich) D/Si(100) surface was exposed to modulated H-beam to induce HD and D<sub>2</sub> desorptions at various  $T_s$ . The H-beam was modulated with a chopper rotating at 0.5 Hz with 0.1s on-and 1.9s off-cycles having a  $\approx 0.02$ s rising-and falling-time. Desorbed species are detected by the QMS in an angle integrated mode. The signal pulses from the QMS were fed into the multi-channel scalar (MCS, 2048 memory, dwell time of 0.9 ms) triggered with the rotating chopper. First 30 or 60 pulses in the train of the pulsed desorption signals were accumulated for HD or D<sub>2</sub> desorption, respectively. Nascent desorption rate spectrum  $F(t)$  can be obtained from the rate equation (3):

$$\frac{dN(t)}{dt} = F(t) - \alpha N(t) \quad (3)$$

where,  $N(t)$  is the raw density data measured by the QMS and  $\alpha$  is the pumping speed of the evacuation system. From the exponential decrease of D<sub>2</sub> gas density injected into the reaction chamber through the same chopper of the H-beam, we obtained  $\alpha = 14.8 \text{ s}^{-1}$  for the uncalibrated gas density measured by the QMS. The validity of the evaluated  $\alpha$  was further confirmed by checking that the modulated D<sub>2</sub> beam profile could be indeed reproduced by Eq.(3). Rest of the details are explained in the Chapter 2.

## 4.2 Pulsed desorption of HD and D<sub>2</sub> molecules

In order to shine characteristic feature of adsorption-induced desorption (AID) reactions, particularly related to the instability of excess dideuteride generated during the H impulse, D<sub>2</sub> desorptions were measured both on dideuteride free and dideuteride rich surfaces. Dideuteride rich saturated surfaces were prepared by 3 minutes D dosing at  $T_s$  below 573K, on the other hand, monodeuteride surfaces were prepared by 1 min D dosing at  $T_s = 573$  K. However, the amount of dideuterides on the saturated surfaces was decreased with  $T_s$  due to  $\beta_2$  TD. Thence, initially prepared dideuteride rich and dideuteride free surfaces were exposed to modulated H beam at different  $T_s$  to reveal the reaction lifetimes of HD and D<sub>2</sub> desorptions by using a short pulsed H beam.

Before accumulating data with the QMS/MCS system, trend of the pulsed HD and D<sub>2</sub> signals were measured. Fig.4.1 shows the HD and D<sub>2</sub> desorption densities measured by the QMS in a pulse counting mode on saturated surface at 503 K. Admission of the pulsed H beam was started at  $t = 0$ . To get a precise pulse shape, extended time profiles for both HD and D<sub>2</sub> rates are shown in the insets. One might notice that the HD rates jump at each on-cycle and drop down quickly at the beam off-cycles. On the other hand, D<sub>2</sub> rates jump rather slowly at each on-cycle and drop down slowly even at the beam off-cycles with longer tails.

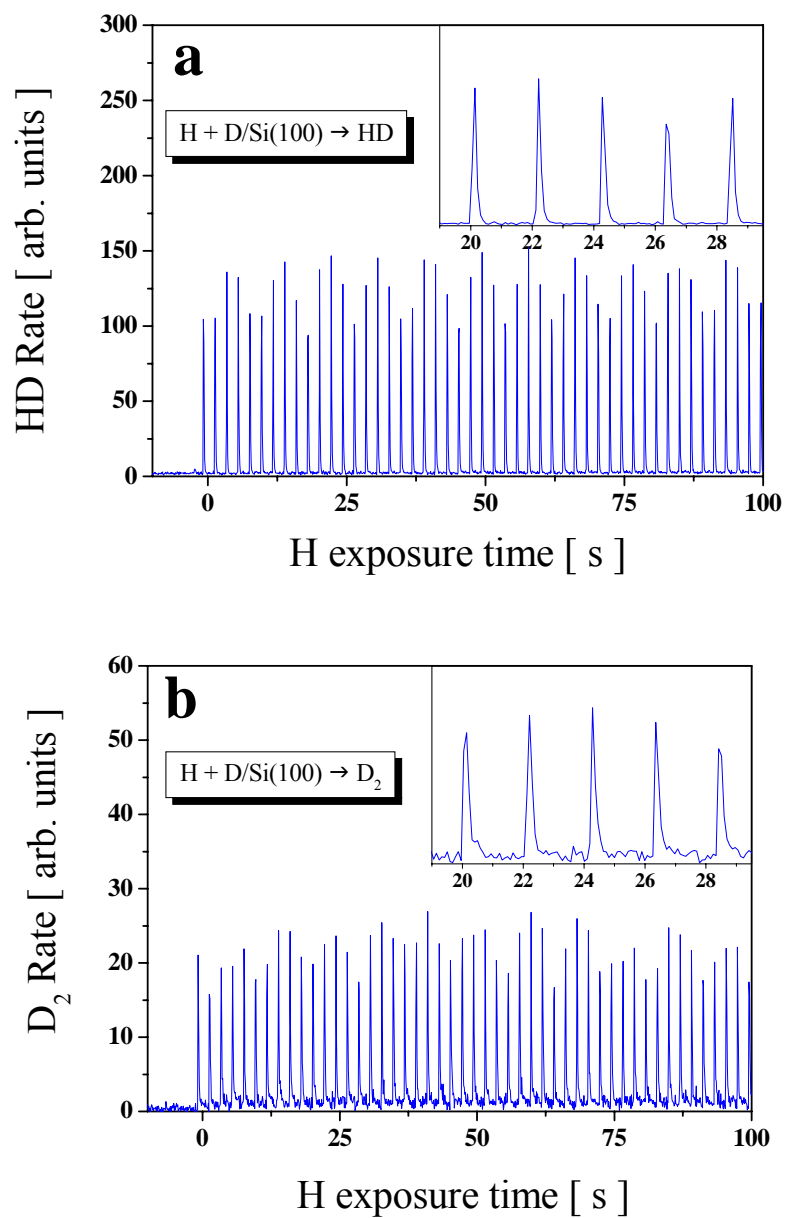


Fig. 4.1 HD (a) and D<sub>2</sub> (b) desorption densities measured with the QMS at 503 K for saturated D/Si(100) surface. The insets show the extended time profile of few cycles.

### 4.3 Reaction lifetime of ABS species

As was reported previously, the desorption yield of HD molecules is approximately proportional to initial D coverages. It is not seriously affected by preexisting dideuterides or transiently formed dideuterides during H irradiation, but slightly decreased with  $T_s$  below 600 K. These facts suggest that the ABS reaction is mostly direct in nature and hence the reaction must be prompt in time. This anticipation was confirmed by analyzing the HD rate curve obtained under the shorter H beam pulse. The nascent desorption rate spectra,  $F(t)$ , were obtained from Eq.(3) after calculating  $dN(t)/dt$  for the measured raw rate curves  $N(t)$ . Fig. 4.2 shows an example of  $F(t)$  as obtained on the 1.0 ML D/Si(100) surface at 573 K. It is obvious that the ABS rate curve is characterized with a steep rise and a steep fall promptly chasing the applied H-impulse. Indeed, the measured ABS rate could be well fit with a single component having the reaction lifetime of 0.005 s as shown in Fig. 4.2. However, one should note that the value of 0.005 s is upper limit because the rise time ( $\approx 0.02$  s) of the used H-impulse is 4 times longer than the evaluated lifetime.

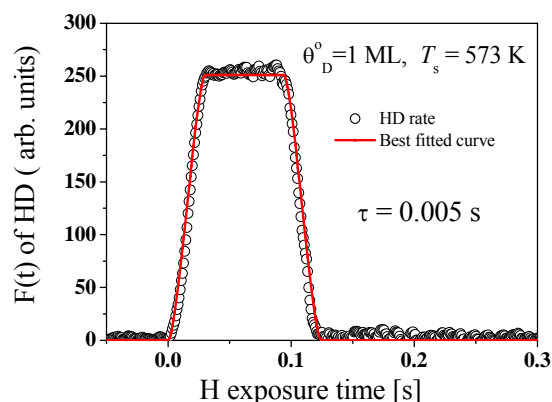


Fig. 4.2 Nascent HD desorption rate curve measured at 573 K for initial D coverage 1 ML on the Si(100) surface. The width of the H impulse is about 0.1 s. The red line is the best fitted curve by Eq. (2) in the text with the parameter of  $\tau = 0.005$  s.

## 4.4 Reaction lifetimes of AID species

The time response of  $D_2$  molecules desorbed along the AID pathway, i.e.,  $H + D/Si(100) \rightarrow D_2$ , was also measured for various  $T_s$  and  $\theta_D'$ . An example of  $D_2$  rate curve measured for  $\theta_D = 1.2$  ML at 503 K is plotted in Fig.4.3. Contrasted to the HD rate curves, the nascent  $D_2$  rate curves are found to be characterized with a slow increase in the on-cycles of the modulated H-beam and a long tail in the off-cycles. This feature observed in time response suggests that the AID desorptions contributed by multiple components. After trial and error analysis according to the Eqs. (1) and (2), the nascent  $D_2$  rate curve,  $F(t)$ , was decomposed into four components, by means of a least mean squares method. I consider that the adsorption of H atoms to the surface kinetically prepare different kinds of surface entities, which are responsible for  $D_2$  emission along an exponential law with a lifetime of  $\tau_i$  ( $i=1-4$ ). Results were plotted in Fig.4.3. The lifetimes of the four components were determined to be  $0.005 \pm 0.001$ ,  $0.06 \pm 0.01$ ,  $0.8 \pm 0.1$ , and  $30 \pm 5$  s, respectively. The reaction lifetime of the shortest component is as short as that of the HD rate, and therefore it should be reminded that the measured lifetime is an upper limit. The rate curves measured in the different conditions for  $T_s$  and  $\theta_D=1$ ML were also decomposed into four components along the same method. Fig.4.4 shows the details of  $D_2$  fitting on 1ML surfaces. As a result, all the rate curves measured at various temperatures and coverages were found to be fit with the same lifetimes as obtained above for the curves plotted in Fig.4.3.



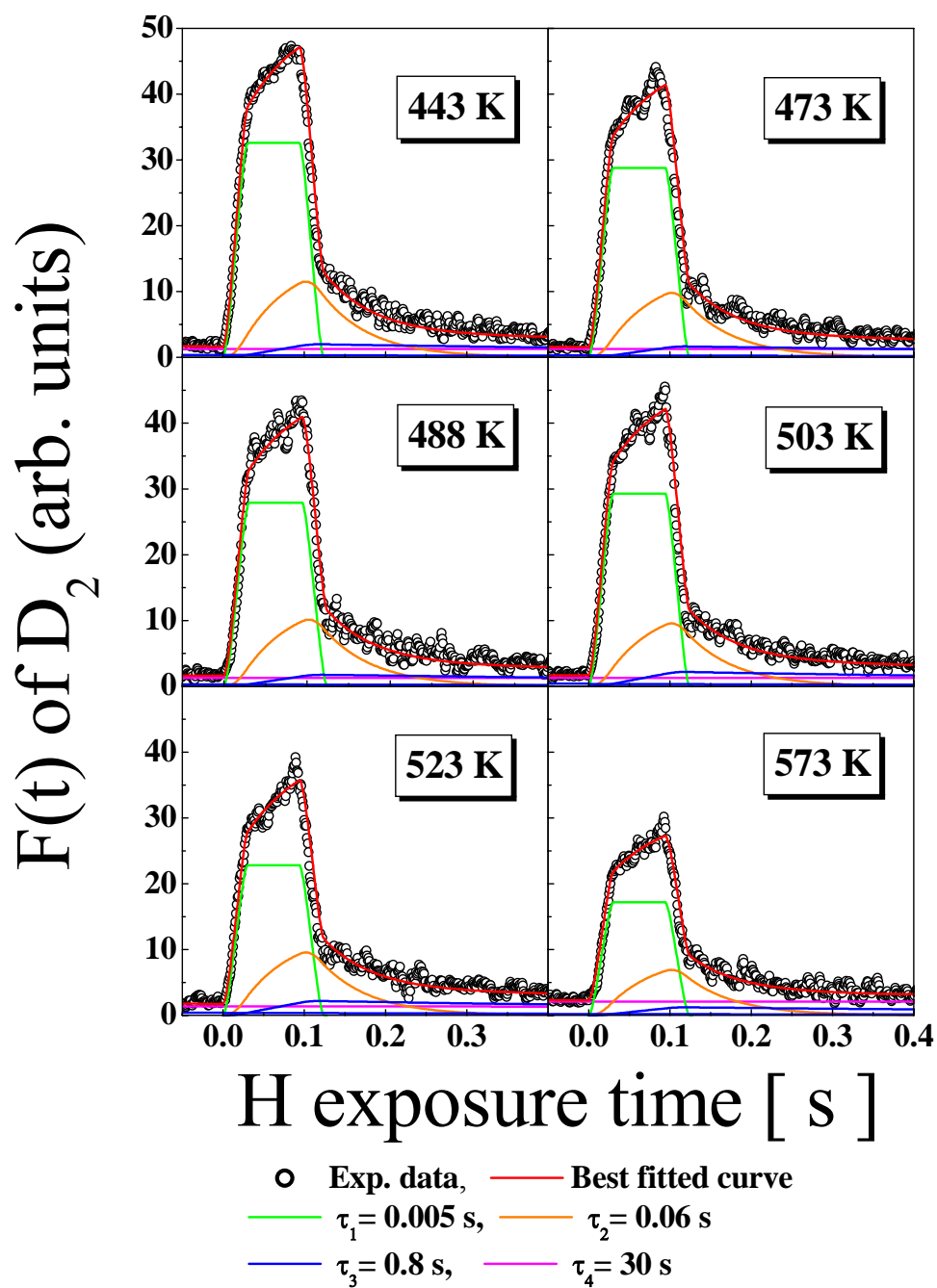
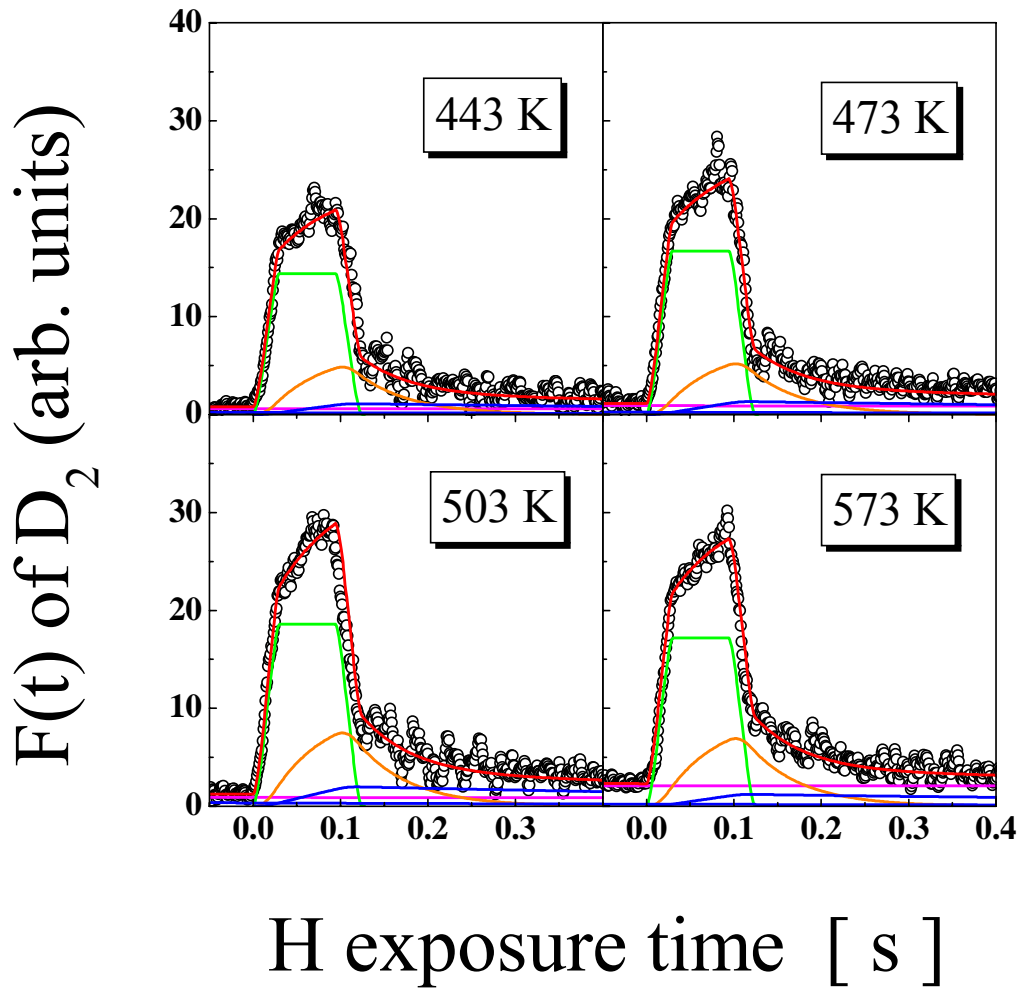


Fig. 4.3 Nascent  $D_2$  rate curves,  $F(t)$ , measured at different  $T$ s for  $\theta_D^0 = 1.2$  ML on the Si(100) surfaces. The rate curves are decomposed into four components with the lifetimes of  $\tau_1 = 0.005$ ,  $\tau_2 = 0.06$ ,  $\tau_3 = 0.8$  and  $\tau_4 = 30$  shown by the different colors.



○ Exp. data, — Best fitted curve  
 —  $\tau_1 = 0.005$  s, —  $\tau_2 = 0.06$  s  
 —  $\tau_3 = 0.8$  s, —  $\tau_4 = 30$  s

Fig. 4.4 Nascent  $D_2$  rate curves,  $F(t)$ , measured at different  $T$ s for  $\theta_D^0 = 1.0$  ML on the Si(100) surfaces. The rate curves are decomposed into four components with the lifetimes of  $\tau_1 = 0.005$ ,  $\tau_2 = 0.06$ ,  $\tau_3 = 0.8$  and  $\tau_4 = 30$  shown by the different colors.

## 4.5 Temperature dependence of AID species

The effect of temperature on the four D<sub>2</sub> components on saturated and monolayer (ML) surface has also been revealed. The intensities of the four components varied depending on both  $T_s$  and  $\theta_D$  as plotted in Figs. 4.5. The left side figure shows the case measured for the initial D coverages saturated at given  $T_s$ , thus containing dideuterides, and the right side figure shows the case for  $\theta_D = 1.0$  ML where no dideuterides were present before H exposure. After analyzing the curves in the two figures, it is clear that, the yield of the longest lifetime ( $\tau_4 = 30$ s) component increase with  $T_s$ . In contrast, in case of other three components, the performance is reverse. This explains that D<sub>2</sub> component showing lifetime  $\tau_4 = 30$ s, is temperature susceptible and will be denoted simply as  $\beta_2$  TD (section 4.6.3). The second point is that, the yield of the four components becomes larger on the D-saturated surfaces than on the 1.0 ML D-covered surface for  $T_s < 500$  K. This suggests that dideuterides, already present before H exposure, increase the D<sub>2</sub> yield, i.e. dideuterides play a significant role in AID. Another significant point is that the yield pattern of slowest component ( $\tau_1 = 0.005$ s). As we mentioned, this is the upper limit of our detected slowest component, hence, more components of D<sub>2</sub> having lifetime below  $\tau_1 = 0.005$ s could be possible and D saturated surface is the fertile area to form these components. On the other hand, the yield is almost stagnant in 1ML surface.

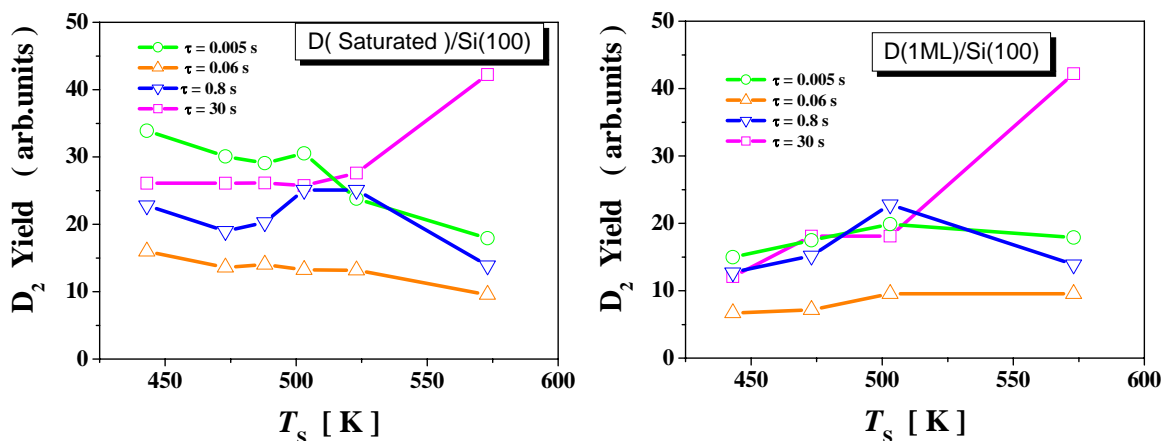


Fig. 4.5 Plots of integrated  $D_2$  yields of four components on saturated and monolayer (ML) surfaces at different surface temperature ( $T_s$ ). In both circumstances, yield of longest lifetime (30s) component increases ( pink line ) with  $T_s$ , whereas, other there components decrease.

## 4.6 Atomistic AID mechanisms

On the basis of the decomposed components, various pathways of AID can be categorized with reaction lifetimes. This observable fact may be comprehended from the thermodynamical point of view for the Si surface phases attained under H exposure. Northrup<sup>3</sup> calculates stability of the H/Si surface phases as a function of H chemical potential ( $\mu_H$ ), which is an adjustable variable controlled by pressure of a H reservoir as well as  $T_s$ . The origin of  $\mu_H$  has been set so that  $SiH_4$  molecules are formed in the reaction system  $4H + Si(100) \rightarrow SiH_4$  without any cost of energy at 0 K. According to his results, if the surface containing system is in equilibrium with a H reservoir, it takes a distinctive phase for a certain range of  $\mu_H$ . There are two critical levels of  $\mu_H$ ,  $\mu(2 \times 1 \mid 3 \times 1)$  ( $= -0.24$  eV) and  $\mu(3 \times 1 \mid 1 \times 1)$  ( $= -0.09$  eV), by which the possible range of  $\mu_H$  is distinguished for each surface phase. A  $(2 \times 1)$  monohydride phase is stable for

$\mu_{\text{H}} \leq -0.24$  eV, a (3x1) monohydride/dihydride phase is stable for  $-0.24$  eV  $\leq \mu_{\text{H}} \leq -0.09$  eV, and a (1x1) dihydride phase is stable for  $\mu_{\text{H}} \geq -0.09$  eV. Hence, the surface coverage is absolutely fixed to 0, 1.0, 1.33 or 2.0 ML depending on  $\mu_{\text{H}}$ . However, in the present case, the surface system is not in equilibrium with the H reservoir and the surface coverage takes a certain intermediate value in between the above fixed values. For instance, during H exposure at  $T_{\text{s}} = 600$  K, the present H flux does not allow to cover the whole surface throughout the (3x1) monohydride/dihydride phase. The surface coverage achieved under H exposure takes a value in the range  $1.0 \text{ ML} < \theta_{\text{H}} < 1.33 \text{ ML}$ . For such an intermediate coverage, the surface consists of (3x1) monohydride/dihydride domains on the (2x1) monohydride surface. Since such a (3x1) monohydride/dihydride phase is unstable at around 600 K, emission of molecules (along the  $\beta_2$  TD channel) may decrease the monohydride/dihydride domains in the off-cycles of the modulated H-beam experiment. Nevertheless, the (3x1) domains may not be fully evacuated at the end of each off-cycles because  $\tau_4$  is longer than the time duration of the off-cycles. One should remember that the present experiments illuminate various AID pathways when (3x1) domains dynamically expand and shrink synchronously chasing the modulated H-beam at on and off-cycles, respectively. This circumstance can be visualized from the Fig.4.6. The ellipses represent the (3x1) domains in the (2x1) surface. During the modulated H-beam experiments, (3x1) domains start increasing in size at the beam on-cycles (a) and at the beam off cycles, (3x1) domains start decreasing by emitting  $\text{D}_2$  molecules (b) In the next on-cycle, it increases again and so on. In the following subsections, we will discuss possible atomistic AID pathways based on the measured reaction lifetimes.

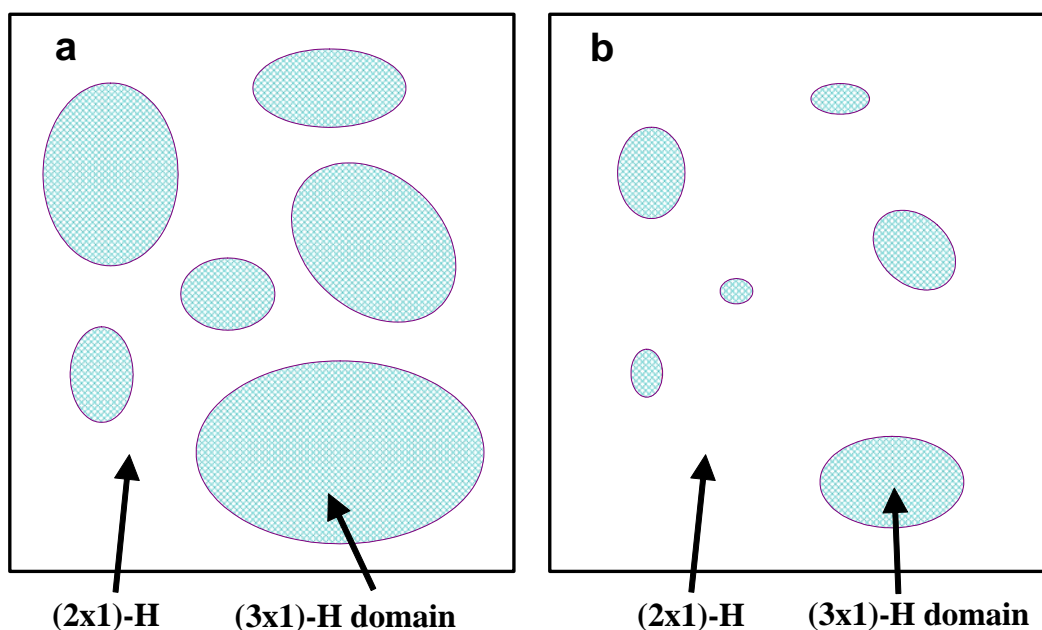


Fig. 4.6 Schematic diagram of (3x1) domains in (2x1) surface. During the modulated H beam experiments, at the H-beam on-cycles, the size of (3x1) domains is larger (a). On the other hand, at the H-beam off-cycles, (3x1) domains start decreasing in size (b) due to emission of  $D_2$  molecules and increase again at the next on-cycle. The number and size of (3x1) domains decrease with H exposure time due to loss of surface D adatoms.

#### 4.6.1 0.005 s and 0.06 s AID species

Northrup assumes that equilibrium of H on the surface is faster than H desorption so that  $\mu_H$  is pinned at  $\mu(2x1 \mid 3x1)$  throughout the Si surface. If otherwise  $\mu_H > \mu(3x1 \mid 1x1)$ , the surface coverage under H exposure exceeds 1.33 ML and thus (1x1) domains are present on the (3x1) surface. In other words, if the surface phases are in equilibrium with each other, three phases, [(2x1), (3x1), and (1x1)] cannot coexist simultaneously on the surface. For example, (1x1) domains locally formed on (3x1) domains on a (2x1) monohydride surface are thermodynamically unstable. Therefore, such (1x1) dihydride domains formed on the (3x1) domains must fade away by emitting molecules so that  $\mu_H$  may be pinned at  $\mu(2x1 \mid 3x1)$ . This implicates

that pinning  $\mu_H$  at  $\mu(2 \times 1 \mid 3 \times 1)$  is the driving force for the fast AID channel. Fig.4.7 shows a ball and stick model which illustrates this fast AID mechanism. At step-1 a H atom is captured by a DSi-SiD cell to form a localized hot complex,  $(H + \text{DSi-SiD})^*$ . As a possible relaxation channel, the DSi-SiD dimer bonds will be broken by H in competition with the ABS. Then, four neighboring dihydrides are arranged as a local  $(1 \times 1)$  domain in the  $(3 \times 1)$  phase at step-2. Since this  $(1 \times 1)$  domain is thermodynamically unstable a  $\text{D}_2$  molecule is emitted and thereby the Si dimer is restored at step-3. The emission of a  $\text{D}_2$  molecule from this configuration does not require any extra displacement of the created dihydrides. Hence this may be responsible for such a fast emission of molecules as observed in the fastest AID with the reaction lifetime of

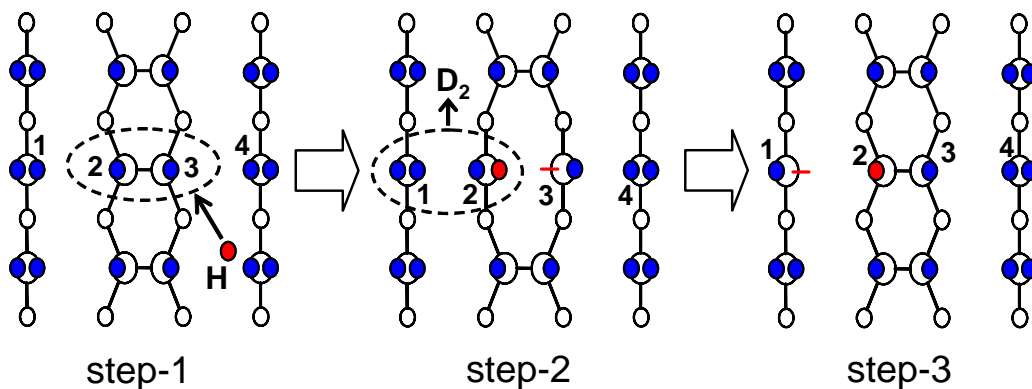


Fig. 4.7 Top view of the ball and stick model to illustrate the mechanism of the fast AID generated on  $(3 \times 1)$  domains at the on-cycles of the H-beam. Blue circles represent D adatoms. Big and small circles represent the first and second layer Si atoms, respectively. A H atom (red) breaks the Si dimer bond (labeled by 2 and 3) in step-1, making four locally adjacent dihydrides (labeled as 1, 2, 3 and 4) in step-2. These four dihydrides are considered as a  $(1 \times 1)$  dihydride domain locally formed on the  $(3 \times 1)$  domain. Such a  $(1 \times 1)$  local domain is thermodynamically unstable toward  $\text{D}_2$  emission which leaves behind an occupied Si dimer (labeled as 2,3) and one dihydride with one dangling bond (red, labeled as 1) in step- 3. Consequently, the original  $(3 \times 1)$  domain is restored.

$\tau_1=0.005$  s. Furthermore, the backbonds of Si atoms (labeled by 2 and 3) are strained by the neighboring Si dimers at step-2. The stress due to this strain and the Si dangling bonds created by breaking the dimer bond further promote the emission of molecule to remake the Si dimer bond at step-3. Relative stability of local (1x1) dihydride domains may be different depending on sites where they are formed. If they are formed close to, e.g., the periphery of the (3x1) domains, surface vacancies, or already existing (1x1) dihydride domains, the four neighboring dihydrides tend to become stabler since the back bond strain is relaxed there to some extent, resulting in the reaction lifetime longer. Thus it may be plausible that the lifetimes of the transient (1x1) domains are distributed depending on the local configurations of the sites where they were formed. The value of  $\tau_2 = 0.06$  s may be understood as an upper bound for the possible fast AID pathways.

#### 4.6.2 0.8 s AID species

The  $D_2$  component characterized with the lifetime of  $\tau_3 = 0.8$  s may be basically categorized to the fast AID. That is, the process occurs also through the instability of four neighboring dihydrides when  $\mu_H$  is pinned at  $\mu(2x1 \mid 3x1)$  for the surface consisting of a mixture of (3x1) and (2x1) phases. Taking the somewhat longer lifetime of  $\tau_3 = 0.8$  s into consideration, four neighboring dihydrides may be formed at a site less strained than those considered above for the fastest AID. As one of the most favorable adsorption sites, we invoke a boundary region in between the (3x1) domains and the (2x1) monohydride phase. This idea was proposed for the first time by Qin and Norton<sup>4</sup>, who suggested that molecules would be emitted as the area of the (3x1)



domains build up under H exposure. The conversion of a (2x1) phase to a (3x1) phase along their model is illustrated with the ball and stick model in Fig.4.8. Dihydrides at the boundaries could be formed by directly breaking the Si dimer bonds by incoming H atoms. Alternatively, dihydrides could be brought at the boundary from the region of (2x1) monohydride phase as a result of surface diffusion. For  $T_s \geq 500$  K, a pair of neighboring dihydrides are energetically unstable because of a repulsive interaction among them due to steric effect between two terminating H atoms. Thence, the dihydrides diffuse across the surface to pile up at the boundaries at step-2 in Fig.4.8. Such dihydrides piled up at the boundary region are energetically unstable and emit a molecule, thereby enlarging (3 x 1) domains under H-beam on-cycles. One can easily

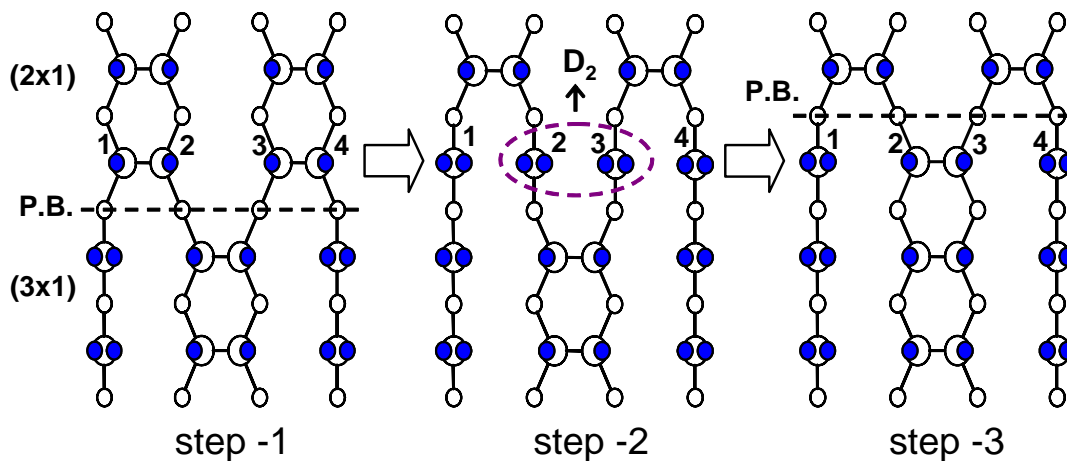


Fig. 4.8 Ball and stick model to illustrate the atomistic mechanism of the  $\tau_3 = 0.8$  s AID generated at the phase boundary between the (3x1) domain and (2x1) surface. This model was given by Qin and Norton for the first time to explain the formation of anti-phase boundary present in between the (3x1) and (2x1) phases.<sup>4</sup> H atoms break the Si dimers as labeled by 1 and 2, and 3 and 4 at step-1 and then four neighboring dihydrides at step-2 are formed. These four adjacent dihydrides are thermodynamically unstable toward molecule emission.  $D_2$  desorption occurs from this local area shown as the dotted ellipse at step-2, leaving behind the Si dimer as labeled by 2 and 3. Consequently, the phase boundary line denoted by P.B. is shifted up by one lattice constant at step-3. Symbols are the same as those defined in Fig. 4.7.

notice that the row of dimer (HSi–SiH) inside the (3x1) domain is shifted upward (step-3 in Fig.4.8) by one row with respect to those in the (2x1) monohydride domains, forming an anti-phase boundary.

### 4.6.3 30 s AID species

Excess surface energy is stored in the enlarged (3x1) monohydride/dihydride domains as the H atoms are admitted onto the surface in the on-cycles of the modulated H-beam. Such excess surface energy must be relaxed in the successive off-cycles of the H-beam by reducing the enlarged (3x1) domain area. The AID path with the lifetime of  $\tau_4 = 30$  s may be attributed to this path. Hence the AID could be considered as a sort of the  $\beta_2$  TD arising from the (3x1) phase. The kinetic experiments<sup>5,6</sup> so far done for the  $\beta_2$  TD revealed that the desorption activation energy is 1.8–2.0 eV, and the molecular desorption obeys a second order rate law in dihydride coverage. The theoretical calculations could reproduce the measured desorption activation energy.<sup>7,8</sup> The most reasonable model to describe the  $\beta_2$  TD may be  $2\text{HSiH} \rightarrow \text{HSi–SiH} + \text{H}_2$ . The two neighboring dihydrides can be brought via an isomerization reaction by which HSi–SiH and HSiH swap their sites in the (3x1) monohydride/dihydride domains. The recent STM experiments<sup>9</sup> supports this  $\beta_2$  TD path. However, this picture may not be straightforwardly applied to the slow AID having the reaction lifetime of  $\tau_4 = 30$  s since it occurs at temperatures even lower than the conventional  $\beta_2$  TD. Furthermore, the reaction lifetime of 30 s is shorter than that of the lifetime of  $\beta_2$  TD ( $\geq 100$  s) below 575 K. [In order to estimate the desorption lifetime for the  $\beta_2$  TD path, we describe its rate constant in a quasi first-order Arrhenius form, i.e.,

$k(T_s) = \nu \cdot \exp(-E_a/kTs)$ , where,  $\nu$  is the pre-exponential factor and  $E_a$  is the activation energy for  $D_2$  desorption. Taking values that  $\nu = 3 \times 10^{14} \text{ s}^{-1}$  and  $E_a = 1.88 \text{ eV}$ ,<sup>10</sup> we obtain rate constant,  $k(575 \text{ K}) = 10^{-2} \text{ s}^{-1}$ , i.e., the desorption lifetime in  $\beta_2$  TD evaluated to be approximately 100 s at 575 K.] We may anticipate that the desorption proceeds basically along the same pathway as for the conventional  $\beta_2$  TD channel, except that it occurs at the periphery of the (3x1) domains rather than their central area. Fig. 4.9 illustrates a possible mechanism to describe the AID channel having the  $\tau_4 = 30 \text{ s}$  reaction lifetime occurring at an anti-phase boundary. Since the tensile stress exerted to the Si lattice through their backbonds at the phase boundary<sup>4,11</sup> may promote such an site-exchanging isomerization reaction between HSi-SiH (DSi-SiD) and H-Si-H (D-Si-D). Then the dihydride labeled with 4 at step-1 in Fig. 4.9 will move to the position labeled 2 to make a pair of dihydrides at step-2. These two dihydrides

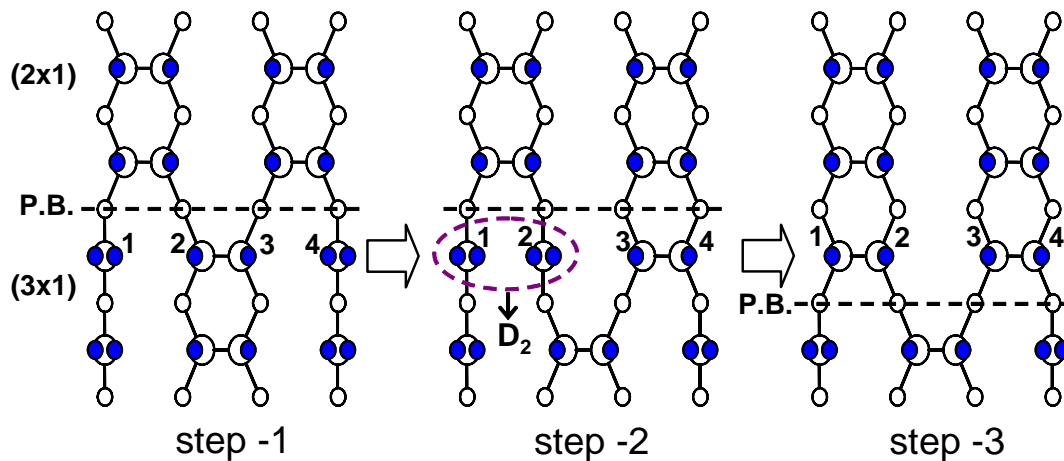


Fig. 4.9 Ball and stick model to illustrate the mechanism of the  $\tau_4 = 30\text{s}$  AID. At step-1, the site exchange reaction takes place via an isomerization reaction between Si dimer labelled as 2 and 3 and a dideuteride labelled as 4, making a pair of adjacent dihydrides at step-2. Instability of the two dihydrides gives rise to emission of one  $D_2$  molecule, leaving behind the doubly occupied dimer at step-3. This decreases the area of the (3x1) domain, shifting the phase boundary (P.B.) by one lattice constant down. Symbols are the same as those in Fig. 4.7.

will undergo the molecular emission leaving behind a monohydride Si dimer of which phase matches to that of the (2x1) monohydride phase. In this way, the phase boundary shifts by one lattice constant to the lower position, thereby resulting in the decrease of the (3x1) domain.

## 4.7 Conclusion

I investigated the transient desorption of HD and D<sub>2</sub> molecules in the reaction system H + D/Si(100). While the HD desorption induced by H atom occurred promptly as a modulated H-beam was admitted onto the D covered Si surface, the D<sub>2</sub> desorption occurred even after the H irradiation was turned off in the off-cycles of the pulsed beam. The D<sub>2</sub> desorption has been understood in terms of the adsorption-induced desorption or AID. The D<sub>2</sub> rate curves were decomposed into four components characterized with the reaction lifetimes of  $\leq 0.005$ ,  $\approx 0.06$ ,  $\approx 0.8$ , and  $\approx 30$  s. These AID paths could be related to the thermal instability of the Si–H(D) surface phases. The fastest and the second fastest AID paths were considered to occur immediately when the (1x1) dihydride (dideuteride) domains are formed by the adsorption of H atoms on the (3x1) domains. On the other hand, the 0.8 s AID path was related to the increase of the (3x1) domains when four neighboring dihydrides are formed at the boundaries between the (3x1) domains and the (2x1) monohydride phase. The slow AID path characterized with the 30 s lifetime was attributed to the thermal desorption from the (3x1) monodeuteride/dideuteride domains, which were excessively formed under H exposure beyond the equilibrium coverage. Thus the slow AID accompanies a phase transition from the (3x1) of (2x1) phase. Ball and stick models were given to illustrate these atomistic mechanisms for the three AID pathways.

## References

---

1. F. Rahman, M. Kuroda, T. Kiyonaga, F. Khanom, H. Tsurumaki, S. Inanaga, A. Namiki, *J. Chem. Phys.* 121 (2004) 3221.
2. S. Inanaga, H. Gotoh, A. Takeo, F. Khanom, H. Tsurumaki, A. Namiki, *Surf. Sci.* 596 (2005) 82.
3. J. E. Northrup, *Phys. Rev. B* 44 (1991) 1419.
4. X. R. Qin, P. R. Norton, *Phys. Rev. B* 53 (1996) 11100.
5. P. Gupta, V. L. Colvin, S. M. George, *Phys. Rev. B* 37 (1988) 8234.
6. M. C. Flowers, N. B. H. Jonathan, Y. Liu, A. Morris, *J. Chem. Phys.* 99 (1993) 7038.
7. P. Nachtigall, K. D. Jordan, C. Sosa, *J. Chem. Phys.* 101 (1994) 8073.
8. M. R. Radeke, E. A. Carter, *Phys. Rev. B* 54 (1996) 11803.
9. S.-S. Ferng, C.-T. Lin, K.-M. Yang, D.-S. Lin, T.-C. Chiang, *Phys. Rev. Lett.* 94 (2005) 196103.
10. S. Inanaga, F. Rahman, F. Khanom, A. Namiki, *J. Vac. Sci. Technol. A* 23 (2005) 1471.
11. Y. Suwa, M. Fujimori, S. Heike, Y. Terada, Y. Yoshimoto, K. Akagi, O. Sugino, T. Hashizume, *Phys. Rev. B* 74 (2006) 205308.